Radionuclide imaging of hypoxia: Where are we now? Special attention to cancer of the cervix uteri

Kgomotso M.G. Mokoala[1] **MD,**
Ismaheel O. Lawal[1,2] **MD, PhD,**
Jae Min Jeong[3,4] **MD, PhD,**
Mike M. Sathekge[*1,2] **MD, PhD,**
Mariza Vorster[1,2] **MD, PhD**

1. Department of Nuclear Medicine, University of Pretoria, Pretoria, South Africa
2. Nuclear Medicine Research Infrastructure (NuMeRI), Steve Biko Academic Hospital, Pretoria, South Africa
3. Radiation Applied Life Sciences, Department of Nuclear Medicine, Institute of Radiation Medicine, Seoul National University College of Medicine, Seoul, Korea
4. Cancer Research Institute, Seoul National University College of Medicine, Seoul, Korea

Keywords: Hypoxia imaging ,- Cervical cancer - PET/CT, - Nitro-imidazole-based tracers, - ^{68}Ga-labelled nitroimidazole

Corresponding author:
Mike M. Sathekge MD, PhD
Department of Nuclear Medicine, University of Pretoria & Steve Biko Academic Hospital, Pretoria, South Africa
Phone: +27 12 354 1794
mike.sathekge@up.ac.za

Received:
14 October 2021
Accepted revised:
14 December 2021

Abstract

Cancer of the cervix is the fourth commonest malignancy in women worldwide and it also ranks fourth as the cause of cancer related mortality in women. Hypoxia is a common characteristic of solid tumours and cervical cancer is no exception. Hypoxia is associated with increased aggressiveness, risk of invasion and metastasis. Tumour hypoxia also results in resistance to both radiation therapy and chemotherapy leading to a poorer prognosis. In-vivo measurement of tumour hypoxia is vital in oncologic practice because it can predict outcome and identify patients with a worse prognosis. Mapping of tumour hypoxia may also help select patients that may benefit from applicable treatments. While traditional methods of measuring hypoxia such as the Eppendorf probe is considered the gold standard, it is invasive and technically demanding. Non-invasive methods of measuring tumour hypoxia are ideal. Positron emission tomography/computed tomography (PET/CT) imaging with nitro-imidazole-based tracers is a highly sensitive nuclear imaging technique that is suited for non-invasive in vivo monitoring of hypoxia. Over the years various hypoxia specific PET tracers have been investigated in various malignancies including cancer of the cervix. Several fluorine-18 (^{18}F)-based tracers have been studied and although most had small patient numbers, the results are promising and generally demonstrate an associate between the presence of hypoxia and treatment outcome. The need for an onsite cyclotron and specialized radiopharmacy skills make these tracers unattractive and largely unavailable for routine clinical applications. With the increase in availability of the gallium-68 (^{68}Ga) generator this makes the ^{68}Ga-labelled nitroimidazole derivatives attractive because ^{68}Ga is available from a generator with a shelf life of almost a year. The chemistry of ^{68}Ga makes for easy labelling with several peptides and molecules. Pre-clinical work has demonstrated the feasibility of using these tracers for imaging hypoxia and has laid the groundwork for further human studies with these tracers. The aim of this review is to discuss hypoxia and its impact in cancer of the cervix as well as to look into the progress made in hypoxia imaging in cancer of the cervix. This will focus on the tracers studied thus far and some of the challenges of hypoxia imaging.

Hell J Nucl Med 2021; 24(3): 247-261 *Published online: 28 December 2021*

Introduction

Cancer of the cervix is the fourth commonest female malignancy in both incidence and mortality, however in middle to lower income countries, it ranks second after breast carcinoma [1]. Although there is no single known causative factor, human papilloma virus (HPV) has been found to be a significant contributor in the pathogenesis of cervical cancer [2-3]. Persistent infection with oncogenic strains of HPV results in progression of cervical cancer pre-cursors to invasive carcinoma [3]. Immunosuppression, especially human immunodeficiency virus (HIV), smoking, sexual behavior, parity, the use of oral contraceptives and diet are other factors that have been associated with an increased risk of cervical cancer [4]. The introduction of vaccination and screening programs has resulted in a decline in the rate of cervical cancer in developed countries [5]. This is something yet to be realized in developing countries.

Tumour microenvironment

Human cancers have a complex cellular environment. This environment is the product of the interactions of the tumour with its host. It consists of tumour cells, the tumour stroma, blood vessels, infiltrating inflammatory cells, fibroblasts and a multitude of other associated cells [6]. The tumour coordinates molecular and cellular events taking place in surrounding tissues [6]. The cellular changes in the tumour microenvironment are responsible for the progression of cancers [7]. The presence of cancer associated fibroblasts (CAF), deregulated extracellular matrix deposition, repression of the immune system and expanded vascularization are some features of the tumour environment

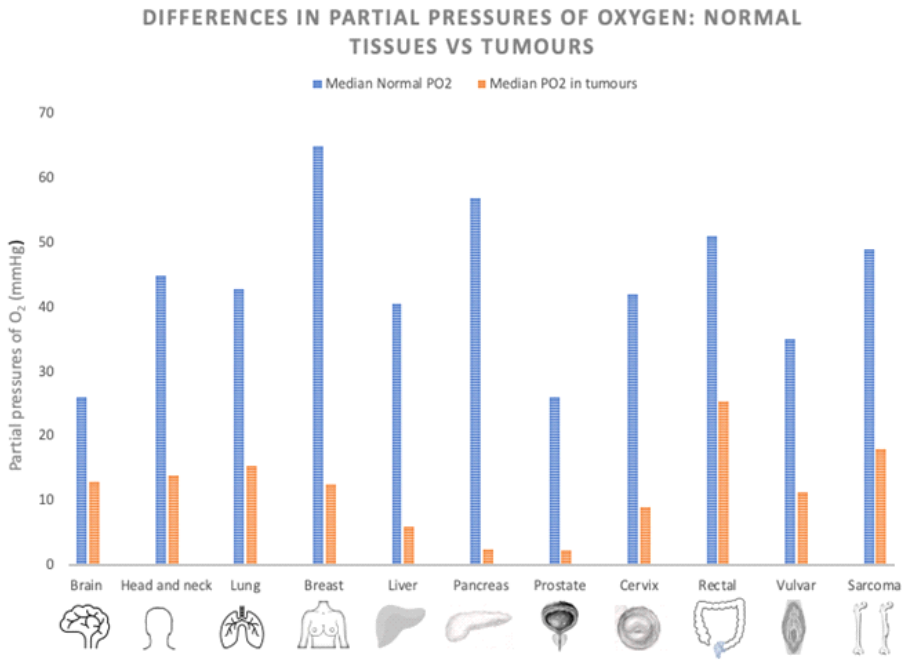

Figure 1. An overview of the Oxygen partial pressures in normal tissue versus tumour tissues in various malignancies that have been investigated for hypoxia.

that lead to progression [7-8].

The differences in the vasculature of normal and malignant cells leads to sluggish and irregular flow in cancer, which results in a supply and demand mismatch [9-10]. These vascular anomalies are responsible for the resultant tumour microenvironment which consists of hypoxia and increased interstitial fluid pressure (IFP) [11].

Hypoxia refers to a state of low oxygen concentration that compromises biologic functions or when the partial pressure of oxygen (pO_2) falls below critical values (<5-10mmHg) [12-13]. In solid tumours, there is an oxygen demand-supply mismatch due to the rapid growth of the tumour cells and the poorly formed new vessels. The causes of hypoxia can be broadly classified as perfusion (acute), diffusion (chronic) or anaemia-related [14].

Another component of the tumour microenvironment is the interstitial fluid pressure (IFP). It is elevated in most solid tumours in comparison with normal tissues. Poor lymphatic drainage decreased interstitial permeability and vascular leakiness result in high IFP values [11,15-17]. In a study of 102 patients with cancer of the cervix, Milosevic et al. (2001) showed that pre-treatment IFP measurements were an independent prognostic factor for recurrence and cause-specific death [17]. They went on to suggest that IFP might be a useful tool to select patients for novel treatment strategies targeted at the tumour vasculature [18]. Studies from other authors support these findings [15,19].

The work by Vaupel and colleagues (2001) offers insight into the oxygenation status of cervical cancer. In pre-therapeutic data from cervix cancers in pre and post-menopausal women, they found that two-thirds of locally advanced squamous cell carcinoma lesions demonstrated heterogeneously distributed hypoxic regions with pO_2<2.5mmHg [20]. In over one hundred tumours, they went on to demonstrate that oxygen tensions differed significantly between the normal cervix of nulliparous women and those with locally advanced cervical cancer (median pO_2: 42mmHg vs 10mmHg respectively) [20]. Hypoxia has been investigated in other types of carcinomas (Figure 1) [21-31].

Clinical significance of hypoxia

Hypoxia can influence proteomic changes that may result in one of two pathways. On the one hand, these changes may result in impaired growth and / or cell death and on the other hand, it may result in adaptations that lead to survival of the cells under hypoxic and nutrient deprived conditions [32]. At different thresholds of oxygen tension, they induce heterogeneous changes by activating different signaling pathways which result in angiogenesis, glycolysis, inhibition of apoptosis and upregulation of growth factors [32].

Several mechanisms are associated with increased risk of metastasis, and these include changes in clonal selection and genomic changes. The clinical implication of these cellular changes is resistance of tumour cells to cancer treatments (radiation therapy and some chemotherapy) [14,33].

Although it may appear that hypoxic tumours do not respond well to any treatment, the resistance of these tumours to radiation therapy is the best understood. As early as the 1920's, the effects of radiation on vegetable seeds were investgated and it was found that a correlation between radiosensitivity and the presence of oxygen exists [34]. During radiation therapy, the presence of oxygen is necessary for the fixation of the DNA damage made by free radicals [34].

Hockel et al. (1996) demonstrated more extensive local disease, more frequent parametrial infiltration and lymphovascular invasion in locally advanced cervix cancer tumours that were more hypoxic compared to tumours that were not [35]. They also went on to show that the 5-year overall survi-

val was significantly reduced for hypoxic tumours as opposed to those that are well oxygenated, regardless of the type of treatment received [35].

Measuring Hypoxia

The measurement of hypoxia in tumours has been the subject of investigation with different methods being developed over the years. The invasive technique with polarographic oxygen electrodes is considered the gold standard. Newer less invasive techniques (direct and indirect) have been developed to overcome the disadvantage of the gold standard. Over the last decade the focus has been on exogenous markers as well as hypoxia-related endogenous markers. Due to the heterogeneity of hypoxia, imaging of hypoxia with single photon emission computed tomography (SPECT), PET and magnetic resonance imaging (MRI) is an exciting area of research interest as it can provide maps of tumour hypoxia to plan radiotherapy. All the techniques available interrogate different aspects of the hypoxic microenvironment and they provide information on hypoxia at different locations. The information on the state of hypoxia may be used to predict treatment outcome and select patients for hypoxia modifying treatment.

Polarographic oxygen needle electrodes

Polarographic electrodes are probes that can be introduced directly into the tissue of interest. A detectable current proportional to the pO_2 is generated at the cathode end due to a reduction in oxygen. The Eppendorf electrode was marketed in the 1980's as an upgrade of the older systems. Pre-clinical and clinical studies have been conducted in a variety of tumours with the Eppendorf probes considered the "gold standard" to validate other new techniques. In an international prospective multicenter trial evaluating the prognostic significance of pre-therapy tumour pO_2 and the hypoxia marker pimonidazole in 127 cervical cancer patients, the authors found that neither of these markers could predict tumour control or overall survival [36]. Other studies found that tumour hypoxia assessed using electrodes was associated with a poor prognosis [23, 37]. The disadvantages of this technique are that it is invasive and cannot be used to map tumour heterogeneity or to repeat measurements on the same site for a long time.

Exogenous markers

In an effort to overcome the limitations of the electrodes exogeneous markers were developed. Two 2-nitroimidazole markers namely pimonidazole (1-[(2-hydroxy-3-piperidinyl)propyl]-2-nitroimidazole hydrochloride) and EF5 ([2-(2-nitro-1H-imidazole-1-yl)-N-(2,2,3,3,3-pentaflou-ropropyl) acetamide]) have been approved for clinical use. Once injected into the bloodstream these markers are reduced and bound to thiol-containing proteins in viable hypoxic cells. In 1999, Raleigh and colleagues found a good correlation between hypoxia measured by pimonidazole and oxygen electrodes measurements as well as the radiobiologically hypoxic fraction in animal models mammary tumour [38]. Clinical studies have found conflicting results with some investigators finding a correlation between the degree of hypoxia estimated by 2-nitroimidazole markers and both locoregional control and event-free survival [39, 40]. Surprisingly most of these analyses were assessing tumours of the head and neck, while the report in cervical cancer patients did not support these findings [24, 25,41]. There have been strides made in this area with a new oral pimonidazole being tested and approved by the FDA. It was found to be convenient, and it permitted the identification of all of the physiologically and therapeutically relevant hypoxic tumour cells.

Endogenous markers

Endogenous markers are proteins upregulated in association with hypoxia and can be measured in blood plasma or immunohistochemically on tumour biopsies.

HIF is a transcription factor, which mediates critical hypoxic adaptations by the induction of target genes involved in glucose metabolism, angiogenesis, erythropoietin and apoptosis. The target genes include vascular endothelial growth factor (VEGF), facilitative glucose transporters (GLUT), hexokinases (HK), erythropoietin (EPO), carbonic anhydrase IX (CAIX/CA9) (Figure 2) [42].

- CAIX / CA9 – Is one of the downstream targets of HIF-1 and it is over expressed in different types of cancers [43-44].
- GLUT1 – Genes that encode for GLUT are upregulated in hypoxic conditions. The two glucose transporters most associated with invasive cancer are GLUT-1 and GLUT-3, being over expressed in cervical carcinoma, head and neck cancer, colorectal and bladder cancer[45].
- VEGF – Plays a crucial role in angiogenesis, physiologically and pathologically in malignant tumour growth [46-47].
- Urokinase Plasminogen Activator (uPA) system – An important signaling route that can enhance the aggressiveness of a tumour [48].
- Osteopontin (OPN) – An integrin-binding protein invol-ved in several physiological processes, such as cytokine production, cell adhesion and migration. Increases the aggressiveness and metastatic potential of tumour cells [49].

The use of the above-mentioned exogenous and endogenous hypoxia markers analyzed in biopsy samples has a few limitations such as invasive sampling, inability to map heterogeneity and the complex regulation of the hypoxia-inducible genes.

Imaging of hypoxia

The ideal properties of an imaging test involve the ability to [50-51]:

1. Distinguish normoxia/hypoxia/anoxia/necrosis.
2. Distinguish between acute (perfusion) related and chronic (diffusion) related hypoxia.
3. Reflect cellular pO_2 as opposed to vascular pO_2.
4. Be applicable to any tumour site with complete loco-regional evaluation.
5. Be simple to perform, non-toxic, non-invasive and allow repeated measurements.
6. Be sensitive at pO_2 levels relevant to tumour therapy.
7. Be predictive of the radiotherapy outcome.
8. Be widely available in imaging centers.

Unfortunately, there is no imaging test that meets all these criteria.

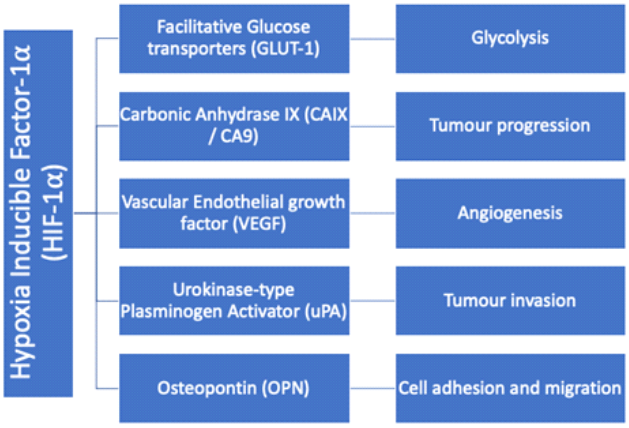

Figure 2. The role of hypoxia inducible factor in the upregulation of transcription factors responsible for tumour aggressiveness and progression.

Magnetic resonance imaging

There are different MRI based methods to non-invasively assess for tumour hypoxia. These include gradient-recalled echo techniques, electron paramagnetic resonance and MR spectroscopy. These techniques are attractive since MRI scanners avoid the complication of short-lived radioactivity and radiation exposure. Further studies are needed to explore whether the different MRI methods may be established as biomarkers of hypoxia and possibly predict treatment outcome. The shortcoming of MRI is the lack of availability.

Single photon emission computed tomography imaging

Single photon emission computed tomography tracers are an attractive option because gamma cameras are more widely available than PET cameras. A few iodine and technetium-99m (^{99m}Tc) labeled tracers have been investigated, however these have not taken off as much as their PET counterparts. This may be related to the superior spatial resolution and more accurate quantitation with PET markers.

Iodine labeled tracers include [^{123}I]I-IAZA and [^{125}I]I-IAZA/^{125}I-iodoazomycin. These tracers show high diffusibility into poorly vascularized ischaemic tissues, high reductive binding rate, moderately rapid blood clearance, rapid total body clearance and minimal loss of radiolabel in animal studies. Several pre-clinical and clinical experiments with the use of these tracers have been carried out [52-53]. In a study by Urtasun et al. (1996), [^{123}I]I-IAZA was found to be feasible and safe. In 51 patients with newly diagnosed malignancies, hypoxia was demonstrated in small cell lung carcinoma and to a lesser degree squamous cell carcinoma of the head and neck. There was no uptake in prostate cancer, melanoma or malignant gliomas [52]. Newer agents based on azomycin-nucleoside structure such as IAG, iodozomycinpyranoside (IAZP), IAZGP and iodozomycinxylopyranoside (IAZXP) have been developed for PET imaging and evaluated with promising results [54-57]. Iodinated azomycin-galactopyranoside (IAZGP) contains the bioreducable moiety 2-nitroimidazole. The higher water solubility and faster clearance from normal tissues result in amended hypoxia detecting properties compared to IAZA [58]. The drawback of these tracers is the cost and the unobtain ability.

Technetium-99m is a very convenient isotope because it is widely available and inexpensive. It has a 6-hour half-life and can be labeled to a variety of tracers. The three most documented [^{99m}Tc]Tc-labeled 2-nitroimidazole tracers for hypoxia imaging are propyleneamine oxime-1,2-nitroimidazole (BMS 181321), oxo[[3,3,9,9-tetramethyl-6-6[(2-nitro-1H-imidazol-1-yl0methyl]5-oxa-4,8-diazadioximato]-(3-)-N,N',N'',N''']technetium (V) (BRU59-21) and 4,9-diaza-3,3,10,10-tetramethyldodecan (HL-91) [59-61]. Data concerning the clinical evaluation of these tracers is limited. The former two tracers have chemical structures based on nitroimidazole and have similar uptake mechanisms while [^{99m}Tc]Tc-HL-91 on the other hand has a poorly understood uptake mechanism. A proposed mechanism of uptake for [^{99m}Tc]Tc-BRU59-21 is metabolism by the NADPH: cytochrome P450 reductase [62]. In pre-clinical work, Melo et al. (2000) compared the difference in uptake between [^{99m}Tc]Tc-BMS 181321 and [^{99m}Tc]Tc-BRU59-21 [63]. They found that the uptake was increased in hypoxic tissues and that [^{99m}Tc]Tc-BRU59-21 had enhanced tumour to muscle ratios because of the more rapid clearance from the blood as compared to [^{99m}Tc]Tc-BMS 181321 [63]. The few clinical studies available look at the use of these tracers in other malignancies with no focus on cervical cancer [64-65]. Despite the favourable properties of ^{99m}Tc, the PET based hypoxia tracers have received much more attention (Figure 3).

PET imaging

The PET hypoxia tracers can be broadly categorized into two groups, fluorine labeled nitroimidazoles and copper labeled diacetyl-bis(N4-methyliosemicarbazone) (ATSM) analogues, however over the past five years, gallium-68 labelled nitroimidazole analogues have been investigated. The mechanism of action of the nitroimidazoles involves passive diffusion across the cell membrane, followed by chemical reduction in a multi-step process mediated by nitroreductase enzymes in the presence of hypoxia. The by-product is highly reactive and binds to macromolecules in the cell thereby fixating the reduced form of tracer intracellularly. In the presence of oxygen, the reductive process is reversed, and no reactive intermediates are formed. The different chemical

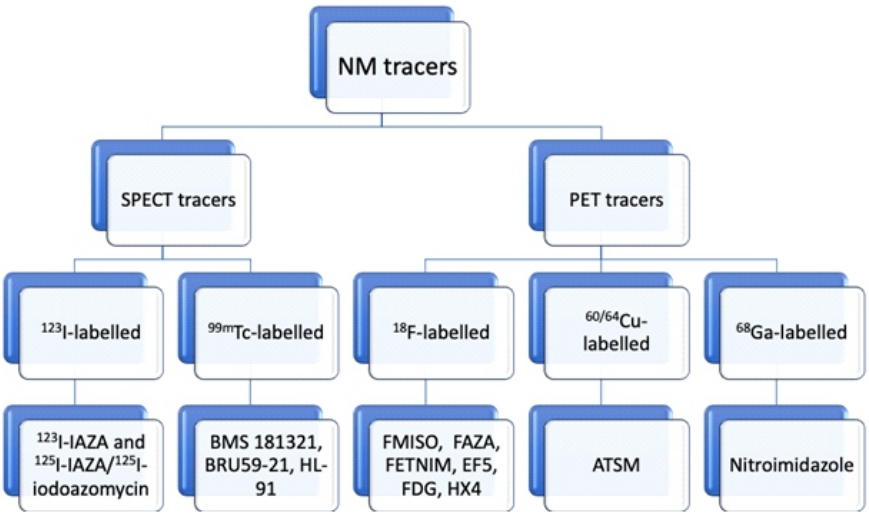

Figure 3. Tracers that have been investigated for both SPECT and PET imaging of hypoxia. Note: Not an exhaustive list of all tracers however this diagram does give a broad indication of the tracers that have been studied).

structure of [$^{64/60}$Cu]Cu-ATSM results in distinctive pharmacokinetic properties that vary from nitroimidazoles.

Fluorine-18 labelled tracers

[^{18}F]F-FMISO

The most extensively investigated PET tracer for hypoxia imaging is ^{18}F-fluoromisonidazole ([^{18}F]F-FMISO). It has the chemical structure of 1-(2'nitro-1'-imidazolyl)-3-fluoro-2 and is usually labelled with fluorine-18 [66]. The precursor for synthesis is usually available commercially. The final product has a purity between 95%-99% and a specific activity between 1 and 3Ci/mol as well as pH between 5 and 8 [66]. Misonidazole is a derivative of the nitroimidazole group of compounds and is administered at sub physiological doses. The biological half-life of misonidazole is 50 minutes [66]. It is a highly lipophilic nitroimidazole tracer with high rates of diffusion across cell membranes. There is slow clearance from normoxic tissues because of the high lipophilicity and these results in a sub-optimal/lowtumour to blood ratio. Long intervals of ±2 hours are required between injection and image acquisitions in order to achieve optimal images, which enable the discrimination between normoxic and hypoxic tissues. This tracer has been expansively studied in a variety of carcinomas; however minimal work has been published on cervical cancer. A pilot study in Austria explored fused multiparametric [^{18}F]F-FMISO/^{18}F-FDG PET and MRI imaging. In all eleven patients, [^{18}F]F-FMISO identified the hypoxic subvolume which was independent of tumor volume [67]. There was a significant strong association between the SUVmax of [^{18}F]F-FDG and [^{18}F]F-FMISO (P=0.04), however the voxel-by-voxel analysis revealed only a weak correlation of these individual parameters. This study is not powered by sufficient numbers to draw strong conclusions; however, the results are promising.

While studies using [^{18}F]F-FMISO have demonstrated significant levels of hypoxia in several cancer types, the routine clinical application of this tracer is lagging behind due to a number of limitations, some of which have been stated above eg. large intra-tumoural uptake variability and poor tumour-to-background uptake etc.

[^{18}F]F-FAZA

It became clear that more hydrophilic compounds are warranted as they may display improved tumour to background ratios. This prompted the Cross Cancer Institute group to develop the sugar coupled 2-nitroimidazole tracer ^{18}F-fluoroazomycin-arabinoside ([^{18}F]F-FAZA) based on the SPECT tracer [^{123}I]I-IAZA, to improve clearance of unbound tracer [68, 69]. In a study comparing the differences in hypoxia detection between [^{18}F]F-FMISO and [^{18}F]F-FAZA, it was shown that [^{18}F]F-FAZA had a lower octanol: water coefficient (log P=1.1) translating to faster tissue and renal clearance [70]. Busk et al. (2008) showed a high correlation between [^{18}F]F-FAZA and the hypoxia exogenous marker pimonidazole in different tumour cell lines, including cervical cancer, in mice [69]. A pilot study in which 15 patients with cervical cancer underwent [^{18}F]F-FAZA PET before, during and three months after therapy (chemoradiation and brachytherapy), showed uptake in only five patients. During therapy only one patient had a negative scan and at 3 months the patient had complete clinical remission, while 4 patients still had positive scans during therapy. Despite positive scans after treatment, only one patient had incomplete remission. This study like most on this subject had a small number of patients therefore the statistical significance of these findings could not be elaborated in detail [71].

[^{18}F]F-FETNIM

As early as 1995, ^{18}F-fluoro-erythronitroimidazole ([^{18}F]F-FETNIM) was synthesized and described by Yang et al. (1995) [72]. This early work showed this tracer to be hydrophilic and have less liver uptake and a predominantly urinary excretory pathway [73]. This tracer has since been explored in various types of cancers, although not much of this data included patients with cervical cancer. A group of investigators decided to look at the feasibility of using this hypoxic tracer in cervical cancer lesions. They compared the hypoxia

images to the metabolic images from the [^{18}F]F-FDG PET/CT study as well as the levels of the tumour markers osteopontin and squamous cell carcinoma. In this limited study the authors demonstrated mild uptake in the primary tumours which proved to be difficult to isolate from the surrounding tissues and therefore discouraging its' use in therapy planning [74]. This is contrary to what others have advocated regarding the other fluorine-18 labelled tracers. Despite their small sample size, they found an association between uptake of tracer and treatment failure as well as prognosis, which is in agreement with other authors [74]. The mean TM ratio in the [^{18}F]F-FMISO cervical cancer study was 2.8 which is higher than that in this [^{18}F]F-FETNIM work, which was two [67, 74]. This finding of higher SUVmax and TB ratios for [^{18}F]F-FMISO was confirmed in a head to head comparison study by Wei and colleagues (2016) in patients with lung cancer [75].

[^{18}F]F-EF5

Immunohistochemical detection of hypoxia with EF5 has been widely used. Fluorine-18-2-(2nitro-1H-imidazol-l-yl)-N-(2,2,3,3,3-pentafluoropropyl)acetamide ([^{18}F]F-EF5) was investigated. In their prospective pilot study of eight patients, Lin et al. (2013) found that [^{18}F]F-EF5 imaging of hypoxia in the uterine cervix is feasible. They acquired images 180 minutes post tracer injection and found a median TM of 1.35. Using this value (1.35) as a cut-off threshold, they found that patients with TM above this threshold had persistent disease and or metastatic disease [76]. The authors admitted that their study was underpowered and the utility of this tracer as well as the predictive value are still to be elucidated. Perhaps the lack of clinical data on this tracer stems from the complexity involved in production of tracer. Despite improvements and simplification of the synthesis of this tracer, it still requires close proximity to a cyclotron and specialized radiopharmacy skills [77, 78].

[^{18}F]F-HX4

Fluorine-18-3-fluoro-2-(4-((2-nitro-1H-imidazol-1-yl) Methyl)-1H-1,2,3,triazol-1-yl)propan-1-ol (HX4)/^{18}F-flortanidazole ([^{18}F]F-HX4) is also a third generation 2-nitroimidazole nucleoside analogue with a 1,2,3-triazole moiety incorporated rendering the compound more hydrophilic than [^{18}F]F-FMISO and [^{18}F]F-FAZA [79]. This increased hydrophilicity results in enhanced renal clearance and improved signal to noise ratios. There was a strong association between [^{18}F]F-HX4 distribution and pimonidazole as well as CA9 positivity in pre-clinical work [79]. In their pre-clinical work, Peeters et al. (2015) made a head-to-head comparison of [18F]F-HX4, [^{18}F]F-FMISO and [^{18}F]F-FAZA and found a higher maximum tumour to background ratio for [^{18}F]F-HX4 when compared to [^{18}F]F-FMISO and [^{18}F]F-FAZA [80]. This finding could not be reproduced in a clinical setting as seen in the work by Chen et al. (2012) who found similar tumour to background ratios for [^{18}F]F-HX4 and [^{18}F]F-FMISO in twelve patients with head and neck squamous cell carcinoma [81]. There has been no published work assessing the utility and feasibility of this tracer in patients with cancer of the cervix. A phase II trial was started, however only four (4) patients were recruited, and the study was terminated due to poor patient participation [79]. Only one study confirmed that high uptake of tracer was negatively correlated with patient outcome in over forty non-small cell lung carcinoma patients [82]. While this tracer is promising, there have been only a few studies to conclusively state whether this tracer performs better than the more robust [^{18}F]F-FMISO.

^{18}F-FDG as a surrogate marker

Imaging with the tracer ^{18}F-FDG has a major role in oncologic imaging. The basis for the use of this tracer is increased glucose metabolism by the cancer cells as a result of aerobic glycolysis, the so-called "Warburg effect" [83]. Anaerobic glycolysis can also occur, and it is due to this that ^{18}F-FDG has been suggested as a surrogate marker of hypoxia. The work of Rajendran et al. (2003) in 49 patients with a variety of malignancies showed no convincing evidence to support the use of ^{18}F-FDG as an indirect marker of hypoxia. They concluded that both [^{18}F]F-MISO and ^{18}F-FDG appear to be complementary, and the combination may be beneficial in the evaluation of solid tumours [84]. This study had few patient numbers, and they included several tumour types in their analysis. This may account for the findings. Studies from Zimny et al. (2006) and Thorwarth et al. (2006) support these findings [85, 86]. Glucose imaging with ^{18}F-FDG cannot reliably differentiate hypoxic from normoxictumours and cannot therefore be used in the place of other more specific tracers.

[$^{60/64}$Cu]Cu-ATSM

There are four available isotopes, namely ^{60}Cu, ^{61}Cu, ^{62}Cu and ^{64}Cu with varying half-lives ranging from 9.7 minutes to 12 hours, however in the context of hypoxia ^{62}Cu and ^{60}Cu are the most studied [87]. High specific activity ^{60}Cu, ^{61}Cu and ^{64}Cu can be produced from a small biomedical cyclotron [88, 89]. Copper-62 may be produced from a Zinc-62/Copper-62 generator which is commercially available [90]. Among the copper radioisotopes, ^{64}Cu is the most commonly used. This is due to the physical characteristics of the isotope which include a half-life of 12.7 hours and decay by positron emission as well as electron capture. The relatively long half-life makes for off-site distribution of this tracer while the decay properties make it an ideal tracer for both imaging and therapy [87].

Copper complexed with thiosemicarbazones was initially developed for myocardial perfusion imaging and later modified to image hypoxia. In a bid to develop alternative tracers to [^{18}F]F-FMISO and fluorine labelled tracers, radioactive copper complexed with diacetyl-bis(N4-methylthiosemicarbazone) (ATSM) was developed by Fujibayashi and colleagues (1997) [91]. After passive diffusion into the cell, [$^{60/64}$Cu]Cu-ATSM is reduced in the cytosol in the presence of nicotinamide adenine dinucleotide phosphate (NADPH) [87]. The reduced Cu(i)-ATSM is unstable and dissociates with resultant trapping in hypoxic cells [92-94]. The uptake is more rapid and the hypoxic/normoxic tissue activity ratio is greater, most likely related to the greater membrane permeability and more rapid blood clearance. It is a neutral lipophilic molecule that is reduced and retained in hypoxic tissues. A great deal of pre-clinical work was done with favourable results. Dehdashti and colleagues (2003) studied [^{60}Cu]Cu-ATSM in 14 women with biopsy proven cervical cancer. With a tumour to muscle (TM) ratio of >3.5 as a cut-off, they were able to discriminate patients that were likely to develop recurrence.

Table 1. *Summary of studies / work on hypoxia imaging in cancer of the cervix using different PET tracers and the results / outcome thereof.*

Tracer	Year	Number of animals/patients	Mean /Median SUVmax	T/M ratio	Outcome of study	Reference
Pre-clinical						
[^{18}F]F-FAZA	2013	3		2 – 3.5	Correlation between spatial distribution of ^{18}F-FAZA and the hypoxia marker pimonidazole	Busk
Clinical						
[^{18}F]F-FMISO	2016	11	3.1 (mean 3.7; range: 2.2 – 6.4)	2.6 (mean 2.8; range: 2.0 – 4.6)	Compared to ^{18}F-FDG and found complementary roles	Pinker
[^{18}F]F-FMISO	2018	13	Not stated	*BL: *TBRpeak 2.7 ± 0.8 (2.0 – 4.6) *TP1: 1.6 ± 0.2 (1.5 – 2.1) *TP2: 1.8 ± 0.3 (1.2 – 2.3) *TP3: 1.7 ± 0.3 (1.4 – 2.1)	Compared to MRI Feasible and provides complementary information of tumour characteristics.	Georg
[^{18}F]F-FAZA	2010	15	Not stated	Range: 1.2 – 3.6	Predictive and prognostic role remains to be clarified.	Schuetz
[^{18}F]F-FETNIM	2012	16	Not stated	Mean 2 (range: 1.3 – 5.4)	T/M > 3.2 linked to treatment failure and adverse prognosis.	Vercellino
[^{18}F]F-EF5	2013	8	Not stated	1.35 (range: 0.88 – 1.79)	T/M >1.35 linked to persistent disease.	Lin

**BL = baseline, *TBRpeak = target to background ratio peak *TP1 = timepoint 1 (week 2 after therapy), *TP2 = timepoint 2 (week 5 after therapy), *TP3 = timepoint 3 (week 19 after the start of therapy).*

The TM ratio was inversely proportional to the progression-free survival (PFS) and the overall survival (OS). No correlation was found between [^{60}Cu]Cu-ATSM uptake and ^{18}F-FDG PET [95]. The same group of authors found similar results in a larger group of patients and even in different malignancies eg rectal and non-small cell carcinoma (NSCC) of the lung [95-98]. A comparison between ^{60}Cu and ^{64}Cu in ten women with cancer of the cervix revealed that both tracers displayed the same pattern and intensity of uptake, however ^{64}Cu had superior image quality [99]. This tracer has reduced renal clearance as compared to the others and thus would be of benefit in pelvic malignancies. The clinical applications of this tracer have been limited due to the high cost of production and the lack of availability. Table 1 summarizes some of the work with various PET tracers.

Gallium-68-labelled tracers

Gallium-68 (^{68}Ga) is a PET tracer with favourable pharmacokinetic characteristics that enable labelling with many peptides and other small molecules. The commercial accessibility of germanium-68/gallium-68 (^{68}Ge/^{68}Ga) generators has stimulated researchers to develop new ^{68}Ga-based radiopharmaceuticals for hypoxia PET imaging. These radiotracers are more hydrophilic than the ^{18}F-labelled tracers resulting in better clearance from background and ultimately higher target to background ratios. Their mechanism of uptake and retention is similar to that of the ^{18}F-labelled tracers (Figure 4). The nitroimidazole compound undergoes an electron reduction inside the cell to form a nitro radical anion. In hypoxic tissue, the nitro radical anion is reduced further to form reactive species that covalently bind to intracellular macromolecules [100].

A group from Korea synthesized nitroimidazole derivates for PET imaging by labelling ^{68}Ga and conjugating with bifunctional chelating agents 1,4,7-triazacyclononane-1,4,7-triacetic acid (NOTA) and isothiocynatobenzyl-NOTA (SCN-NOTA) via ethyleneamine bridge by formation of amide and thiourea bonds [101]. There was a high labelling efficiency (>96%) and the compounds were stable at room temperature and at 37°C in human serum [101]. The uptake of both products was increased under hypoxic conditions. Biodistribution studies showed increased tumour to muscle ratios in animal studies. They found that [^{68}Ga]Ga-NOTA-NI was more hydrophilic and had higher T/M ratios than [^{68}Ga]Ga-NOTA-SCN-NI [101]. The same group further synthesized two nitroimidazole derivatives by conjugating nitroimidazole and 1,4,7,10-tetraazacyclododecane-1,4,7,10-tetraacetic acid (DOTA) via an amide and a thiourea bond. High labelling efficiencies were achieved when labelled with ^{68}Ga. The products had low partition coefficients (^{68}Ga-4: log P=-4.6; ^{68}Ga-5: log P=-4.5) providing proof of the hydrophilic nature. Both derivatives displayed high uptake in mouse colon cancer cell lines cultured under hypoxic conditions as opposed to under normoxic conditions [102].

In 2012, Fernandez and colleagues contrived two 5-nitroimidazole derivatives, 10-[2-(2-methyl-5-nitro-1-H-imidazole-1-yl)ethylaminocarbonylmethyl]-1,4,7,10-tetrazacyclododecane-1,4,7-triacetic acid (Nit1) and 10-{[N-methyl-1-[1-

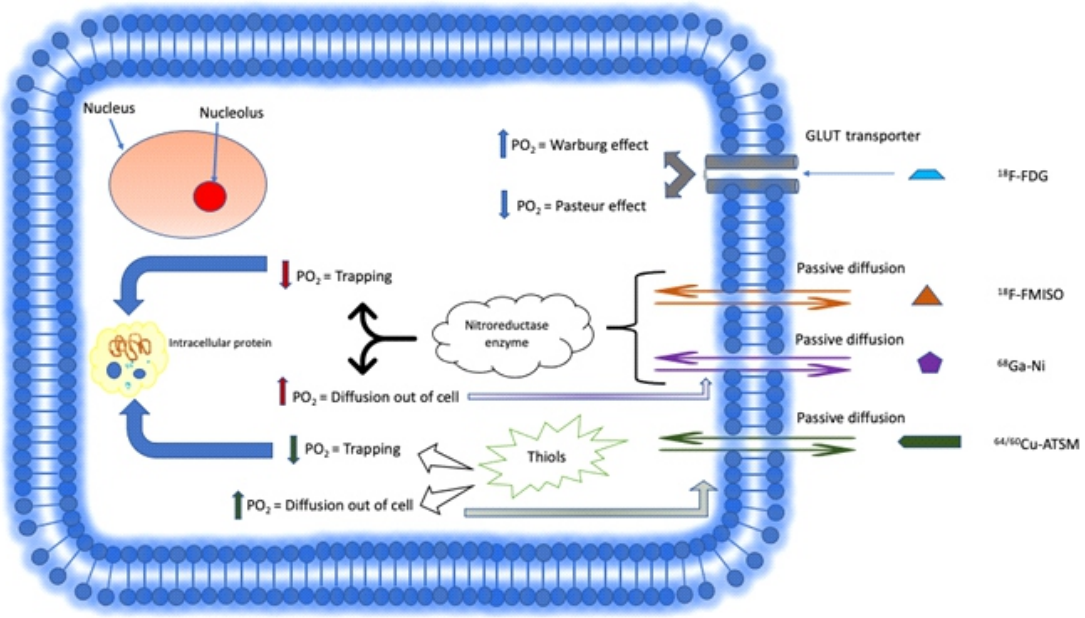

Figure 4. An illustration of the different groups / categories of tracers that have been investigated for imaging hypoxia and their mechanism of entry and trapping in the cells. ^{18}F-FDG enters the cell via the glucose transporters which are upregulated in hypoxic environments. Fluorine-18-FMISO and ^{68}Ga-nitroimidazole tracers enter the cell through passive diffusion and are reduced by the nitroreductase enzymes. In hypoxic environments they become trapped and bind to intracellular proteins. In well ventilated tissues, the tracers diffuse out of the cell. $^{64/60}$Cu-ATSM also enters through passive diffusion and binds to thiols within the cell and becomes trapped in hypoxic environments similar to the other tracers. PO_2 – partial pressure of oxygen; GLUT – glucose transporter.

(2-(2-methyl-5nitro-1 H-imidazole-1-yl)ethyl)-1 H-1,2,3-triazole-4-yl] methylaminocarbonylmethyl}-1,,4,7,10-tetraazacyclododecane-1,4,7-triacetic acid (Nit2) [103]. Both these products were stable in human serum for ±2 hours and had high uptake in hypoxic tissue. In this study, [^{18}F]F-FMISO was tested under the same experimental conditions, and it was found that findings were comparable [103].

The nitroimidazole derivative of HP-DO3A (HP-DO3A-NI) also demonstrated stability when complexed with ^{68}Ga. It is structurally similar to [^{68}Ga]Ga-DOTA-NI, thermally stable, small in size and electrically neutral making for easy diffusion across cell membranes [104]. In vitro studies showed accumulation of this agent in hypoxic tissues at all time points studied (30, 60 and 120 minutes). The in-vivo studies in mice bearing lung carcinoma at 2 hours revealed T/M ratio of 5.0±1.2 [104]. As expected, there was predominant genitourinary excretion with negligible tracer accumulation in the liver, heart and lung.

Other chelators that were investigated were acyclic hexadentate (N_4O_2) chelator, 1,2-[[6-carboxypyridin-2-yl]methylamino]ethane (H_2dedpa) and chiral derivative H_2CHXdedpa (CHX=cyclohexyl/cyclohexane. The H_2CHX dedpa incorporates a 1R,2R-transcyclohexanediamine back-bone in place of the ethylenediamine bridge to form a different ligand [105]. The compounds were radiolabelled with ^{67}Ga and ^{68}Ga. In vitro uptake studies in three cancer cell lines (colon, breast and Chinese hamster ovarian) were performed and showed that all the derivates have preferential uptake in hypoxic cells with T/M ratios as high as 7.9±2.7 at 2 hours [105]. No in-vivo studies were conducted; therefore, this may be an area for future research.

Modified 2-nitroimidaole was labelled to bifunctional chelating agents 1,4,7,10-tetrazacyclododececane,1-(glutaric acid)-4,7,10-triacetic acid (DOTAGA) and 1,4,7-triazacyclododececane,1-(glutaric acid)-4,7-diacetic acid (NODAGA) to produce 2-NIM-DOTAGA and 2-NIM-NODAGA [106]. Biodistribution and PET studies were performed in Swiss mice bearing fibrosarcoma. Assessment was done at 180 minutes post incubation and demonstrated hypoxia selectivity by both complexes although slightly lower for [^{68}Ga]Ga-DOTAGA-2-NIM [106]. The NODAGA chelator displayed more favourable pharmacokinetics and tumour accumulation compared with DOTAGA and [^{18}F]F-FMISO in the same animal model [106].

It is clear that different chelators do not significantly alter the properties of ^{68}Ga labelled nitroimidazoles. Regardless of the chelator used, the ^{68}Ga labelled nitroimidazoles are preferentially taken up in hypoxic tissue and may be used for mapping tumour hypoxia [100,104-106]. To the best of our knowledge, there have been no human studies exploring the use of these ^{68}Ga-labelled nitroimidazole derivatives. This is an area yet to be explored. In a recent review, the potential for imaging hypoxic TB lesions using these tracers was discussed and further highlights the need for more clinical studies in this area to fully explore the potential of these tracers [107]. It would also be of interest to see how these tracers perform in cancer of the cervix and other cancer entities overall, especially since most of the work has shown these tracers to perform better than [^{18}F]F-FMISO [101-103,106].

Table 2 gives a summary of pre-clinical work with [^{68}Ga]Ga-nitroimidazoles.

Clinical Implications for hypoxia imaging

The work on PET imaging of hypoxia has demonstrated a strong association between uptake of tracer and prognosis. A meta-analysis published on studies assessing PET hypoxia

Table 2. *Summary of the pre-clinical work with gallium-68 labelled nitroimidazole derivatives and the findings.*

Tracer	Chelator	Cell lines	PET studies	Mean SUVmax (1 hour post tracer)	Tumour to muscle ratio SUV ratios	Time of evaluation	Year	Ref
[^{68}Ga]Ga-HP-DO3A-nitroimidazole	HP-DO3A	A549 non-small cell carcinoma	Yes		5.1 ± 0.7 (at 120min)	120 min	2015	Wu et al.
[^{68}Ga]Ga-NOTA-nitroimidazole	NOTA	CHO CT-26	Yes	0.30 ± 0.2	5.7 ± 2.5	60 min	2010	Hoigebazar et al.
[^{68}Ga]Ga-SCN-NOTA-nitroimidazole	SCN-NOTA	CHO CT-26	Yes	0.19 ± 0.1	3.95 ± 1.3	60 min	2010	Hoigebazar et al.
[^{68}Ga]Ga-TRAP-nitroimidazole	TRAP	U87MG CT-26	Yes	^{68}Ga-3: 0.10 ±0.06 ^{68}Ga-4: 0.20 ± 0.06 ^{68}Ga-5: 0.33 ± 0.08 ^{68}Ga-6: 0.59 ± 0.09	^{68}Ga-3: 2.97 ± 0.01 ^{68}Ga-4: 3.50 ± 0.02 ^{68}Ga-5: 4.12 ± 0.06 ^{68}Ga-6: 7.41 ± 1.12	60 min	2015	Seelam et al.
[^{68}Ga]Ga-DOTA-nitroimidazole	DOTA	CT-26	Yes	0.53 ± 0.1	5.64 ± 0.8	60 min	2011	Hoigebazar et al.
[^{68}Ga]Ga-SCN-DOTA-nitroimidazole	DOTA-SCN	Hela, CHO, and CT-26	Yes	0.17 ± 0.1	3.83 ± 0.8	60 min	2011	Hoigebazar et al.
[^{68}Ga]Ga-H_2dedpa-nitroimidazole	H_2dedpa	HT-29, LCC6HER-2 CHO	No	N/A	N/A	120 min	2015	Ramogida et al.
[^{68}Ga]Ga-H_2CHXdedpa-nitroimidazole	H_2CHXdedpa	HT-29, LCC6HER-2 CHO	No	N/A	N/A	120 min	2015	Ramogida e al.
[^{68}Ga]Ga-DOTA-nitroimidazole	DOTA	C57 (3LL) HCT-15	No	N/A	N/A	30, 60 and 120 min	2012	Fernandez et al.
[^{68}Ga]Ga-DOTAGA-2-NIM	DOTAGA	CHO	No	N/A	N/A	30, 60 and 180 min	2021	Mittal et al.
[^{68}Ga]Ga-NODAGA-2-NIM	NODAGA	CHO	No	N/A	N/A	30, 60 and 180 min	2021	Mittal et al.

**CHO - Chinese hamster ovarian, CT-26 – Mouse colon cancer, Hela – Henrietta Lacks cervical cancer, C57 (3LL) – Lewis carcinoma, HCT-15 (CCL-225TM ATCC) – Human adenocarcinoma.*

NOTA: 1,4,7-Triazacyclononane-1,4,7-triacetic acid

DOTA: 1,4,7,10-tetraazacyclododecane-1,4,7,10-tetraacetic acid

- *[^{68}Ga]Ga-NOTA-2-NI-N-ethylamine, ^{68}Ga-SCN-NOTA-2-NI-N-ethylamine*
- *TRAP: 1,4,7-triazacyclononane-1,4,7-tris[methyl(2-car- boxyethyl)phosphinic acid]*
- *[^{68}Ga]-Ga3: ^{68}Ga-1,4,7-triazacyclononane-1,4,7- tris[methyl(2-carboxyethyl)phosphinic acid]*
- *[^{68}Ga]Ga-4: ^{68}Ga-3-((7-mono ((hydroxy(3-(2-(2-nitroimidazolyl)ethylamino)-3-oxopropyl)phos- phoryl)methyl)-1,4,7-triazonane -1,4-[methyl(2-carboxyethyl) phosphinic acid]*
- *[^{68}Ga]Ga-5: ^{68}Ga-3-(((4,7-bis((hydroxy(3-(2-(2-nitroimida- zolyl)ethylamino)-3-oxopropyl)phosphoryl)methyl)-1,4,7-triazo- nane-1-[methyl(2-carboxyethyl)phosphinic acid]*
- *[^{68}Ga]Ga-6: ^{68}Ga-1,4,7-triazonane-1,4,7-triyl(tris(methylene)tris(3-(2-(2-nitroimidazolyl) ethylamino)-3-oxopropylphosphinic acid*

DOTA nitroimidazoles:

- *[^{68}Ga]Ga-1: ^{68}Ga-10-[2-(2-methyl-5-nitro-1 H-imidazole-1-yl)ethylaminocarbo- nylmethyl]-1,4,7-tris(tert-butoxycarbonylmethyl)-1,4,7,10-tetraazacyclo-dodecane-1,4,7-acetate*
- *[^{68}Ga]Ga-2: ^{68}Ga-10-{[N-methyl-1-[1-(2-(2-methyl-5-nitro-1 H-imi- dazole-1-yl)ethyl)-1 H-1,2,3-triazole-4yl]methylaminocarbonylmethyl}- 1,4,7,10-tetraaza-cyclododecane-1,4,7-acetate*
- *[^{68}Ga]Ga-3: ^{68}Ga-2-(2-Nitroimidazolyl)ethylamine-DOTA*
- *[^{68}Ga]Ga-4: ^{68}Ga-2-(2-Nitroimidazolyl)ethylamine-SCN-Bz-DOTA*

tracers showed a negative correlation between higher uptake and outcome, with patients with higher uptake having poorer outcome/response to therapy [108]. This has been a consistent trend throughout most published data on hypoxia imaging in cervical cancer. This has resulted in proposals that hypoxia imaging be used to prognosticate patients and to help select patients that may benefit from hypoxia specific drugs. Clinical trials have been undertaken to assess the efficacy of hypoxia-activated prodrugs such as PR-104, TH-302 and EO9 [109-113]. Drugs that target HIF are also available [114]. None of these drugs have shown consistent clinical benefit however their importance in the management of solid malignancies with a potential for hypoxia cannot be ignored. One of the major impediments in the routine application of these drugs is the ability to select patients that will benefit from these drugs, hence the need for hypoxia specific imaging.

The presence of oxygen in tumours enhances the response to radiotherapy with regions containing high oxygen levels being highly amenable to therapy by conventional X-rays. Intensity modulated radiotherapy (IMRT) refers to the ability to produce isodose distribution capable of delivering different dose prescriptions to multiple target sites with extremely high dose gradients between tumour and normal tissues [115]. Closely related to IMRT is the concept of "dose painting", which refers to the targeting of radioresistant areas or areas at risk of relapse (defined by functional imaging) by delivering varied doses of radiation within the tumour [116, 117]. The use of hypoxia imaging may help identify hypoxic subvolumes that may be targeted for improved outcomes in radiotherapy. This leads to personalization of therapy.

Challenges with hypoxia imaging in cancer of the cervix

The search for the ideal tracer for imaging hypoxia has been marred with countless challenges, including tracer properties, ideal imaging time, image analysis and application into routine clinical practice. While the non-exhaustive list above speaks to general challenges in hypoxia imaging, imaging of hypoxia in cervical cancer lesions also has its own challenges. A recent review cited some of these issue amongst others and highlighted the need for further trials in this area to address the application in radiotherapy planning and decision making [118].

Tracer properties

The search for the tracer that ticks all the boxes regarding ease of production, specificity, applicability across a wide range of tumour types and ability to predict radiotherapy outcome, to name a few, is still ongoing. The trade-off for hydrophilicity which improves target to background ratios, is the resultant reduction in uptake in the tumour lesion. This has been the consistent trend as seen with [^{18}F]F-FMISO which is more lipophilic but has better uptake within lesions. While the newer generation tracers have improved target to background ratios, they still trail behind [^{18}F]F-FMISO with regards to uptake in the primary lesion. This is not to say the newer generation of tracers are not of value, this just highlights the challenge of a developing a "perfect or near perfect" tracer.

Ideal imaging time

There is no standard imaging time prescribed for hypoxia imaging. This is understandable due to the variable tracer kinetics. The different tracers all display variable rates of uptake in tumours and washout from the background tissues, thus making standardization challenging. Over and above this is the fact that hypoxia is dynamic, so perhaps dynamic imaging followed by delayed static imaging may offer more insight into this process. Thorwarth et al. (2013) demonstrated the importance of kinetic analysis [119, 120]. While studies involving gliomas, head and neck cancers and lung cancer demonstrated that delayed imaging time revealed a higher target to background at the risk of increased noise, this is not quite the case in cancer of the cervix which is affected by uptake in the adjacent urinary bladder, which is the excretory route of the more hydrophilic tracers. The timing of the scan is of utmost importance as transient hypoxia may be missed.

Image analysis

There is no regularization when it comes to image analysis in hypoxia imaging. In most of the published work, there is a use of qualitative and semi-quantitative parameters to describe and quantify the presence of hypoxia in tumour lesions. Qualitative analysis mostly involves a visual analysis of uptake in the lesion compared to normal surrounding tissue. In most cases the grading will be from 0 meaning no uptake to 3 which is uptake markedly more than the background. Areas with a visual score of 2 and 3 are considered positive for hypoxia [71,121]. The semi-quantitative parameters are the most reported in most studies and they include standardized uptake value maximum (SUVmax), SUVmean, tumour to muscle ratio (TMR), tumour to blood ratio (TBR) and in some cases a hypoxic tumour volume is stated. Of these parameters the most robust is the TMR. Throughout the literature various authors have attempted to come up with a threshold TMR above which there is a certain correlation with patient outcome or prognosis. These vary from 1.35 with [^{18}F]F-EF5 to 3.5 with [^{60}Cu]Cu-ATSM. This may just be a consequence of the differences in the tracers used across studies or may be related to observer variability. In cancers in other regions of the body, there has been a debate regarding the placing of the region of interest for the background, but this has not been the case with cervical cancers as most authors used a spherical region of interest in the thigh or gluteal muscle. This has somewhat harmonized this aspect of the analysis.

Validity of PET hypoxia imaging

Validation is the act of confirming if something is correct or checking if something is accurate. There are limited studies validating the PET tracers as markers of regional hypoxia. This is probably due to the inherent heterogeneous nature of hypoxia which results in incongruities between oxygen electrode sampling and imaging. This is also related to the fact that oxygen electrodes measure hypoxia at the interstitial level while hypoxia PET tracers measure intracellular hypoxia. This is evident from studies reporting mixed correlations between tracer uptake and oxygen electrode measu-

rements in various types of tumours [85,122-124]. Other studies have attempted to correlate PET findings with immunohistochemical staining of exogenous or endogenous markers of hypoxia [74, 95, 96]. These studies have yielded varying results. This may be because staining relies on tissue biopsies which may not always be representative of the tumour and hypoxia distribution within the tumour.

Cervical cancer specific challenges

While [^{18}F]F-FMISO has a more hepatobiliary excretory pathway, the more hydrophilic tracers tend to have predominantly urinary excretion. This creates a huge challenge when imaging hypoxia in tumours located in the pelvis. To circumvent this, some authors have utilized Furosemide at different time points in the imaging protocol. Whether this has made a great impact is uncertain as numbers of participants in most studies is small and the authors do not discuss the diuretic effect in great length. The use of catheters is another viable option to ensure that the bladder is empty at the time of imaging. While it may be easier and more convenient for the patient to void voluntarily prior to image acquisition, however, in most cervical cancer lesions, there is significant incomplete emptying of the bladder. This bladder activity may hamper on visualization of uptake in the tumour lesions which in hypoxia imaging tends to be low to moderate uptake due to tracer kinetics. Perhaps one of the ways to improve analysis in hypoxia imaging of cervical cancer is to acquire dynamic imaging immediately post tracer injection prior to significant drainage in the bladder. There have been no studies dedicated to optimization of imaging as well as analysis protocol in this area. This is an area that needs fine tuning in order to advance hypoxia imaging.

Future perspectives

While there have been significant strides in exploring and identifying novel tracers that are specific for hypoxia, none of the tracers have found their way into routine clinical practice. All tracers thus far have limitations as discussed above. In view of this there is still room for other agents or newer probes to be investigated. Some of these newer agents may be surrogate markers or older tracers that have been chemically modified. One such modification is the synthesis of nitroimidazole derivatives labelled with ^{18}F using an aluminum complex (Al^{18}F-NODA-nitroimidazole) [125].This product demonstrated ease of production as well as lower protein binding which resulted in rapid clearance from blood and non-target tissues and equally rapid uptake in the target tissues [125]. A review by Lyng et al.(2017) proposed combination of imaging modalities such as MRI, CT and PET, to interrogate the tumour microenvironment [126]. This may certainly be the direction to consider, provided there is availability of resources.

Carbonic anhydrase IX

Carbonic anhydrase IX (CA IX) has minimal to no expression in most body organs except the gastrointestinal tract. There has been abnormal expression of CA IX noted in cancers of the brain, kidney, lung, breast, uterine and cervix [127, 128]. Upregulation of the genes that encode for CA IX is best seen in environments that are hypoxic or anoxic [129]. This enzyme expressed on the cell surface is implicated in the progression of cancer and is associated with a poor prognosis. Several attempts have been done to label sulphonamides to ^{18}F or ^{68}Ga for identifying patients who may benefit from treatments targeting this protein (anti-CAIX therapy) or serving as an indirect marker of hypoxia. While antibodies are preferred for identifying potential treatment regimens, smaller molecules are better served for identifying/imaging hypoxic regions within the tumour. In a biodistribution study of four volunteers, Doss et al. (2010), reported that [^{18}F]F-VM4-037 had highest uptake in the liver and kidneys and therefore cannot be used to image these two organs [130, 131]. There was good clearance of the tracer with minimal residual background activity which may result in improved visualization of metastatic hypoxic tissue in various organs (lung and head and neck) and lymph nodes [130, 131]. Prospects for imaging CA IX overexpression in tumours within the pelvis including cervical cancer lesions, are high because of the low retention in the urinary bladder [132, 133]. The pre-clinical work on various cancer cell lines displayed minimal uptake which brings into question their clinical applicability [132, 133]. No clinical data is available regarding their performance in various cancer types and investigating this may present another piece in the puzzle of hypoxia imaging.

Gallium-68 labelled fibroblast activation protein inhibitor

Stromal cells are an essential component of the tumour microenvironment and cancer associated fibroblasts (CAF) constitute ±80% of these cells [7]. These fibroblasts may promote angiogenesis and epigenetic alteration, therefore promoting the growth and metastatic potential of tumour cells [134]. It has been shown that hypoxia induces activation of CAF as well as HIF-1 activated fibroblasts [7,135]. The reprogramming of progenitor cells into CAF's is increased in the presence of hypoxia due to the release of paracrine signaling molecules. TGFb, bFGF and PDGF-B are regulated by HIF-1 [7]. Kugeratski and colleagues (2019) demonstrated that hypoxia exacerbated the pro-angiogenic functions of CAF's [135]. Fibroblast activation protein (FAP) belongs to a family of non-classical serine proteases. It is selectively expressed in activated fibroblasts and sarcomas and is thus found on the surface of these CAF's. The search for anticancer drugs led to the development of FAP-specific inhibitors which of late have been investigated as tumour-targeting radiopharmaceuticals namely [^{68}Ga]Ga-FAPI [136-138]. Early work on this tracer has demonstrated impressive uptake in various cancer types including cervical cancer [137]. Tracers such as [^{18}F]F-FDG imaging have been postulated to be indirect markers of hypoxia, therefore it may not be implausible to hypothesize that [^{68}Ga]Ga-FAPI may also serve as a surrogate marker of hypoxia, based on the mechanism explained above. This tracer is appealing in that the peptide may be radiolabeled with ^{68}Ga, ^{18}F and recently a SPECT version of this tracer has been produced and studied. This could prove to be an interesting area for future research.

In conclusion, it is well known that cervix cancer lesions are hypoxic with resultant aggressiveness and resistance to most forms of therapy, but more so radiation therapy and some forms of chemotherapy. Over the past three decades,

there have been continued efforts to investigate the tumour microenvironment and map hypoxia. While there is a "gold standard" method of assessing tumour hypoxia, it is not without challenges and has not been able to be applied in routine clinical practice. The more attractive options of nuclear medicine imaging of hypoxia have immense potential; however, they all fall short of characteristics of the ideal hypoxia imaging tracer. Thus far the most promising tracer in cancer of the cervix is [$^{60/64}$Cu]Cu-ATSM because of its reduced renal clearance and high tumour uptake; however, the hypoxia selectivity may be questioned as studies failed to show the correlation between tracer uptake and hypoxia immunohistochemical staining. This should encourage researchers to continue the search for the best tracer which is both specific and does not require complex production techniques. At this point even surrogate markers of hypoxia may be sought if they offer the promise of ease of production and accessibility. For lesions in the pelvis a tracer that has minimal renal clearance would be ideal. The newer ^{68}Ga tracers may bridge the gap for introduction of hypoxia imaging in routine clinical practice. The impact of hypoxia imaging has been highlighted and perfecting this aspect of assessment of the tumour microenvironment is key to personalizing therapy.

Bibliography

1. Bray F, Ferlay J, Soerjomataram I et al. Global cancer statistics 2018: Globocan estimates of incidence and mortality worldwide for 36 cancers in 185 countries. *CA Cancer J Clin* 2018; 68(6): 394-424.
2. Humans IWGotEoCRt. Iarc monographs on the evaluation of carcinogenic risks to humans. Ingested nitrate and nitrite, and cyanobacterial peptide toxins. *IARC Monogr Eval Carcinog Risks Hum* 2010; 94:v-vii, 1-412.
3. Bosch FX, de Sanjose S, Castellsague X. Human papilloma virus: Oncogenic risk and new opportunities for prevention. *An Sist Sanit Navar* 2001; 24(1): 7-13.
4. Duarte-Franco E, Franco EL. Cancer of the uterine cervix. *BMC Womens Health* 2004; 4 Suppl 1:S13.
5. Pimple SA, Mishra GA. Global strategies for cervical cancer prevention and screening. *Minerva Ginecol* 2019; 71(4): 313-20.
6. Whiteside TL. The tumor microenvironment and its role in promoting tumor growth. *Oncogene* 2008; 27(45): 5904-12.
7. Petrova V, Annicchiarico-Petruzzelli M, Melino G, Amelio I. The hypoxic tumour microenvironment. *Oncogenesis* 2018; 7(1): 10.
8. Petrova VS, Barlev NA. Tumor microenvironment regulation by hypoxia-indicible factors (HIFS), and p53 family proteins. *Tsitologiia* 2017; 59(4): 259-70.
9. Brown JM, Giaccia AJ. The unique physiology of solid tumors: Opportunities (and problems) for cancer therapy. *Cancer Res* 1998; 58(7):1408-16.
10. Grunt TW, Lametschwandtner A, Staindl O. The vascular pattern of basal cell tumors: Light microscopy and scanning electron microscopic study on vascular corrosion casts. *Microvasc Res* 1985; 29(3): 371-86.
11. Chaudary N, Pintilie M, Schwock J et al. Characterization of the tumor-microenvironment in patient-derived cervix xenografts (OCICX). *Cancers (Basel)* 2012; 4(3): 821-45.
12. Hockel M, Vaupel P. Tumor hypoxia: Definitions and current clinical, biologic, and molecular aspects. *J Natl Cancer Inst* 2001; 93(4): 266-76.
13. Challapalli A, Carroll L, Aboagye EO. Molecular mechanisms of hypoxia in cancer. *Clin Transl Imaging* 2017; 5(3): 225-53.
14. Vaupel P, Mayer A, Hockel M. Tumor hypoxia and malignant progression. *Methods Enzymol* 2004; 381: 335-54.
15. Lunt SJ, Kalliomaki TM, Brown A et al. Interstitial fluid pressure, vascularity and metastasis in ectopic, orthotopic and spontaneous tumours. *BMC Cancer* 2008; 8: 2.
16. Fyles A, Milosevic M, Pintilie M et al. Long-term performance of interstial fluid pressure and hypoxia as prognostic factors in cervix cancer. *Radiother Oncol* 2006; 80(2): 132-7.
17. Milosevic M, Fyles A, Hedley D et al. Interstitial fluid pressure predicts survival in patients with cervix cancer independent of clinical prognostic factors and tumor oxygen measurements. *Cancer Res* 2001; 61(17): 6400-5.
18. Milosevic MF, Pintilie M, Hedley DW et al. High tumor interstitial fluid pressure identifies cervical cancer patients with improved survival from radiotherapy plus cisplatin versus radiotherapy alone. *Int J Cancer* 2014; 135(7): 1692-9.
19. Rofstad EK, Galappathi K, Mathiesen BS. Tumor interstitial fluid pressure-a link between tumor hypoxia, microvascular density, and lymph node metastasis. *Neoplasia* 2014; 16(7): 586-94.
20. Vaupel P, Kelleher DK, Hockel M. Oxygen status of malignant tumors: Pathogenesis of hypoxia and significance for tumor therapy. *Semin Oncol* 2001; 28 (2 Suppl 8): 29-35.
21. McKeown SR. Defining normoxia, physoxia and hypoxia in tumours-implications for treatment response. *Br J Radiol* 2014; 87 (1035): 20130676.
22. Carreau A, El Hafny-Rahbi B, Matejuk A et al. Why is the partial oxygen pressure of human tissues a crucial parameter? Small molecules and hypoxia. *J Cell Mol Med* 2011; 15(6): 1239-53.
23. Nordsmark M, Overgaard J. Tumor hypoxia is independent of hemoglobin and prognostic for loco-regional tumor control after primary radiotherapy in advanced head and neck cancer. *Acta Oncol* 2004; 43(4): 396-403.
24. Nordsmark M, Loncaster J, Chou SC et al. Invasive oxygen measurements and pimonidazole labeling in human cervix carcinoma. *Int J Radiat Oncol Biol Phys* 2001; 49(2): 581-6.
25. Nordsmark M, Loncaster J, Aquino-Parsons C et al. Measurements of hypoxia using pimonidazole and polarographic oxygen-sensitive electrodes in human cervix carcinomas. *Radiother Oncol* 2003; 67(1):35-44.
26. Koong AC, Mehta VK, Le QT et al. Pancreatic tumors show high levels of hypoxia. *Int J Radiat Oncol Biol Phys* 2000; 48(4): 919-22.
27. Vaupel P, Schlenger K, Knoop C, Hockel M. Oxygenation of human tumors: Evaluation of tissue oxygen distribution in breast cancers by computerized O2 tension measurements. *Cancer Res* 1991; 51(12): 3316-22.
28. Vaupel P, Schlenger K, Hoeckel M. Blood flow and tissue oxygenation of human tumors: An update. *Adv Exp Med Biol* 1992; 317: 139-51.
29. Vaupel P, Mayer A, Hockel M. Oxygenation status of primary and recurrent squamous cell carcinomas of the vulva. *Eur J Gynaecol Oncol* 2006; 27(2): 142-6.
30. Vaupel P, Mayer A, Briest S, Hockel M. Hypoxia in breast cancer: Role of blood flow, oxygen diffusion distances, and anemia in the development of oxygen depletion. *Adv Exp Med Biol* 2005; 566: 333-42.
31. Vaupel P, Hockel M, Mayer A. Detection and characterization of tumor hypoxia using pO_2 histography. *Antioxid Redox Signal* 2007; 9(8): 1221-35.
32. Vaupel P. The role of hypoxia-induced factors in tumor progression. *Oncologist* 2004; 9 Suppl 5: 10-7.
33. Vaupel P, Thews O, Hoeckel M. Treatment resistance of solid tumors: Role of hypoxia and anemia. *Med Oncol* 2001; 18(4): 243-59.
34. Hall EJ, Giaccia AJ. Radiobiology for the radiologist. 6th ed. Philadelphia: Lippincott Williams & Wilkins; 2006.
35. Hockel M, Schlenger K, Aral Bet al. Association between tumor hypoxia and malignant progression in advanced cancer of the uterine cervix. *Cancer Res* 1996; 56(19): 4509-15.
36. Nordsmark M, Loncaster J, Aquino-Parsons C et al. The prognostic value of pimonidazole and tumour pO_2 in human cervix carcinomas after radiation therapy: A prospective international multicenter study. *Radiother Oncol* 2006; 80(2): 123-31.

37. Knocke TH, Weitmann HD, Feldmann HJ et al. Intratumoral pO_2-measurements as predictive assay in the treatment of carcinoma of the uterine cervix. *Radiother Oncol* 1999; 53(2): 99-104.
38. Raleigh JA, Chou SC, Arteel GE, Horsman MR. Comparisons among pimonidazole binding, oxygen electrode measurements, and radiation response in c3h mouse tumors. *Radiat Res* 1999; 151(5): 580-9.
39. Evans SM, Koch CJ. Prognostic significance of tumor oxygenation in humans. *Cancer Lett* 2003; 195(1): 1-16.
40. Kaanders JH, Bussink J, van der Kogel AJ. Clinical studies of hypoxia modification in radiotherapy. *Semin Radiat Oncol* 2004; 14(3): 233-40.
41. Kaanders JH, Wijffels KI, Marres HA et al. Pimonidazole binding and tumor vascularity predict for treatment outcome in head and neck cancer. *Cancer Res* 2002; 62(23): 7066-74.
42. Semenza GL. Hypoxia-inducible factor 1 and cancer pathogenesis. *IUBMB Life* 2008; 60(9): 591-7.
43. Airley R, Loncaster J, Davidson S et al. Glucose transporter glut-1 expression correlates with tumor hypoxia and predicts metastasis-free survival in advanced carcinoma of the cervix. *Clin Cancer Res* 2001; 7(4):928-34.
44. Liao SY, Darcy KM, Randall LM et al. Prognostic relevance of carbonic anhydrase-ix in high-risk, early-stage cervical cancer: A gynecologic oncology group study. *Gynecol Oncol* 2010; 116(3): 452-8.
45. Macheda ML, Rogers S, Best JD. Molecular and cellular regulation of glucose transporter (glut) proteins in cancer. *J Cell Physiol* 2005; 202(3): 654-62.
46. Ferrara N, Gerber HP, Le Couter J. The biology of VEGF and its receptors. *Nat Med* 2003; 9(6): 669-76.
47. Moon EJ, Brizel DM, Chi JT, Dewhirst MW. The potential role of intrinsic hypoxia markers as prognostic variables in cancer. *Antioxid Redox Signal* 2007; 9(8): 1237-94.
48. Dass K, Ahmad A, Azmi ASet al. Evolving role of UPA/UPAR system in human cancers. *Cancer Treat Rev* 2008; 34(2): 122-36.
49. Rittling SR, Chambers AF. Role of osteopontin in tumour progression. *Br J Cancer* 2004; 90(10): 1877-81.
50. Mees G, Dierckx R, Vangestel C, Van de Wiele C. Molecular imaging of hypoxia with radiolabelled agents. *Eur J Nucl Med Mol Imaging* 2009; 36(10): 1674-86.
51. Fleming IN, Manavaki R, Blower PJ et al. Imaging tumour hypoxia with positron emission tomography. *Br J Cancer* 2015; 112(2): 238-50.
52. Urtasun RC, Parliament MB, McEwan AJ et al. Measurement of hypoxia in human tumours by non-invasive spect imaging of iodoazomycin arabinoside. *Br J Cancer Suppl* 1996; 27:S209-12.
53. Wiebe E, Denny L, Thomas G. Cancer of the cervix uteri. *Int J Gynaecol Obstet* 2012; 119 Suppl 2:S100-9.
54. Zanzonico P, O'Donoghue J, Chapman JD et al. Iodine-124-labeled iodo-azomycin-galactoside imaging of tumor hypoxia in mice with serial micropet scanning. *Eur J Nucl Med Mol Imaging* 2004; 31(1): 117-28.
55. Riedl CC, Brader P, Zanzonico PB et al. Imaging hypoxia in orthotopic rat liver tumors with iodine 124-labeled iodoazomycin galactopyranoside pet. *Radiology* 2008; 248(2): 561-70.
56. Riedl CC, Brader P, Zanzonico P et al. Tumor hypoxia imaging in orthotopic liver tumors and peritoneal metastasis: A comparative study featuring dynamic ^{18}F-MISO and ^{124}I-IAZG PET in the same study cohort. *Eur J Nucl Med Mol Imaging* 2008; 35(1): 39-46.
57. O'Donoghue JA, Guillem JG, Schoder H et al. Pilot study of PET imaging of ^{124}I-iodoazomycin galactopyranoside (IAZGP), a putative hypoxia imaging agent, in patients with colorectal cancer and head and neck cancer. *EJNMMI Res* 2013; 3(1):42.
58. Iyer RV, Haynes PT, Schneider RFet al. Marking hypoxia in rat prostate carcinomas with beta-d-[^{125}I]azomycin galactopyranoside and [Tc-99m]HL-91: Correlation with microelectrode measurements. *J Nucl Med* 2001; 42(2): 337-44.
59. Kusuoka H, Hashimoto K, Fukuchi K, Nishimura T. Kinetics of a putative hypoxic tissue marker, technetium-99m-nitroimidazole (BMS181321), in normoxic, hypoxic, ischemic and stunned myocardium. *J Nucl Med* 1994; 35(8): 1371-6.
60. Okada RD, Nguyen KN, Strauss HW, Johnson G, 3rd. Effects of low flow and hypoxia on myocardial retention of technetium-99m BMS181321. *Eur J Nucl Med* 1996; 23(4): 443-7.
61. Okada RD, Johnson G, 3rd, Nguyen KN et al. ^{99m}Tc-HL91. Effects of low flow and hypoxia on a new ischemia-avid myocardial imaging agent. *Circulation* 1997; 95(7): 1892-9.
62. Melo T, Ballinger JR, Rauth AM. Role of nadph: Cytochrome p450 reductase in the hypoxic accumulation and metabolism of BRU59-21, a technetium-99m-nitroimidazole for imaging tumor hypoxia. *Biochem Pharmacol* 2000; 60(5): 625-34.
63. Melo T, Duncan J, Ballinger JR, Rauth AM. Bru59-21, a second-generation ^{99m}Tc-labeled 2-nitroimidazole for imaging hypoxia in tumors. *J Nucl Med* 2000; 41(1): 169-76.
64. Cook GJ, Houston S, Barrington SF, Fogelman I. Technetium-99m-labeled HL91 to identify tumor hypoxia: Correlation with fluorine-18-FDG. *J Nucl Med* 1998; 39(1): 99-103.
65. Li L, Yu J, Xing L et al. Serial hypoxia imaging with ^{99m}Tc-HL91 spect to predict radiotherapy response in nonsmall cell lung cancer. *Am J Clin Oncol* 2006; 29(6): 628-33.
66. Xu Z, Li XF, Zou H et al. ^{18}F-fluoromisonidazole in tumor hypoxia imaging. *Oncotarget* 2017; 8(55): 94969-79.
67. Pinker K, Andrzejewski P, Baltzer P et al. Multiparametric ^{18}F-fluorodeoxyglucose/ [^{18}F]fluoromisonidazole positron emission tomography/ magnetic resonance imaging of locally advanced cervical cancer for the non-invasive detection of tumor heterogeneity: A pilot study. *PLoS One* 2016; 11(5): e0155333.
68. Busk M, Mortensen LS, Nordsmark M et al. PET hypoxia imaging with faza: Reproducibility at baseline and during fractionated radiotherapy in tumour-bearing mice. *Eur J Nucl Med Mol Imaging* 2013; 40(2): 186-97.
69. Busk M, Horsman MR, Jakobsen S et al. Imaging hypoxia in xenografted and murine tumors with ^{18}F-fluoroazomycin arabinoside: A comparative study involving micropet, autoradiography, pO_2-polarography, and fluorescence microscopy. *Int J Radiat Oncol Biol Phys* 2008; 70(4):1202-12.
70. Piert M, Machulla HJ, Picchio M et al. Hypoxia-specific tumor imaging with ^{18}F-fluoroazomycin arabinoside. *J Nucl Med* 2005; 46(1): 106-13.
71. Schuetz M, Schmid MP, Potter R et al. Evaluating repetitive ^{18}F-fluoroazomycin-arabinoside (^{18}FAZA) PET in the setting of MRI guided adaptive radiotherapy in cervical cancer. *Acta Oncol* 2010; 49(7): 941-7.
72. Yang DJ, Wallace S, Cherif A et al. Development of F-18-labeled fluoroerythronitroimidazole as a PET agent for imaging tumor hypoxia. *Radiology* 1995; 194(3): 795-800.
73. Gronroos T, Eskola O, Lehtio K et al. Pharmacokinetics of [^{18}F]FETNIM: A potential marker for PET. *J Nucl Med* 2001; 42(9): 1397-404.
74. Vercellino L, Groheux D, Thoury A et al. Hypoxia imaging of uterine cervix carcinoma with ^{18}F-FETNIM PET/CT. *Clin Nucl Med* 2012; 37(11): 1065-8.
75. Wei Y, Zhao W, Huang Y et al. A comparative study of noninvasive hypoxia imaging with ^{18}F-fluoroerythronitroimidazole and ^{18}F-fluoromisonidazole pet/ct in patients with lung cancer. *PLoS One* 2016; 11(6): e0157606.
76. Lin LL, Pryma D, Koch C, Evans S. A pilot study of ^{18}F-EF5 PET/CT imaging in patients with carcinoma of the cervix. *Pract Radiat Oncol* 2013; 3(2 Suppl 1): S26-7.
77. Dolbier WR, Jr., Li AR, Koch CJ et al. ^{18}F-EF5, a marker for PET detection of hypoxia: Synthesis of precursor and a new fluorination procedure. *Appl Radiat Isot* 2001; 54(1): 73-80.
78. Chitneni SK, Bida GT, Dewhirst MW, Zalutsky MR. A simplified synthesis of the hypoxia imaging agent 2-(2-nitro-1h-imidazol-1-yl)-n-(2,2,3,3,3-[^{18}F]pentafluoropropyl)-acetamide ([^{18}F]EF5). *Nucl Med Biol* 2012; 39(7): 1012-8.
79. Sanduleanu S, Wiel A, Lieverse RIY et al. Hypoxia pet imaging with [^{18}F]-HX4-a promising next-generation tracer. *Cancers (Basel)* 2020; 12(5): 1322.

80. Peeters SG, Zegers CM, Lieuwes NG et al. A comparative study of the hypoxia PET tracers [^{18}F]HX4, [^{18}F]FAZA, and [^{18}F]FMISO in a preclinical tumor model. *Int J Radiat Oncol Biol Phys* 2015; 91(2): 351-9.
81. Chen L, Zhang Z, Kolb HC et al. ^{18}F-HX4 hypoxia imaging with pet/ct in head and neck cancer: A comparison with ^{18}F-FMISO. *Nucl Med Commun* 2012; 33(10): 1096-102.
82. Reymen BJT, van Gisbergen MW, Even AJG et al. Nitroglycerin as a radiosensitizer in non-small cell lung cancer: Results of a prospective imaging-based phase ii trial. *Clin Transl Radiat Oncol* 2020; 21: 49-55.
83. Kim BW, Cho H, Chung JY et al. Prognostic assessment of hypoxia and metabolic markers in cervical cancer using automated digital image analysis of immunohistochemistry. *J Transl Med* 2013; 11: 185.
84. Rajendran JG, Wilson DC, Conrad EU et al. [^{18}F]FMISO and [^{18}F]FDG pet imaging in soft tissue sarcomas: Correlation of hypoxia, metabolism and vegf expression. *Eur J Nucl Med Mol Imaging* 2003; 30(5): 695-704.
85. Zimny M, Gagel B, DiMartino E et al. FDG-a marker of tumour hypoxia? A comparison with [^{18}F]fluoromisonidazole and pO_2-polarography in metastatic head and neck cancer. *Eur J Nucl Med Mol Imaging* 2006; 33(12): 1426-31.
86. Thorwarth D, Eschmann SM, Holzner F et al. Combined uptake of [^{18}F]FDG and [^{18}F]FMISO correlates with radiation therapy outcome in head-and-neck cancer patients. *Radiother Oncol* 2006; 80(2): 151-6.
87. Vavere AL, Lewis JS. Cu-atsm: A radiopharmaceutical for the pet imaging of hypoxia. Dalton Trans 2007; (43): 4893-902.
88. McCarthy DW, Shefer RE, Klinkowstein RE et al. Efficient production of high specific activity ^{64}Cu using a biomedical cyclotron. *Nucl Med Biol* 1997; 24(1): 35-43.
89. McCarthy DW, Bass LA, Cutler PD et al. High purity production and potential applications of copper-60 and copper-61. *Nucl Med Biol* 1999; 26(4): 351-8.
90. Fukumura T, Okada K, Suzuki H et al. An improved ^{62}Zn/^{62}Cu generator based on a cation exchanger and its fully remote-controlled preparation for clinical use. *Nucl Med Biol* 2006; 33(6): 821-7.
91. Fujibayashi Y, Taniuchi H, Yonekura Y et al. Copper-62-ATSM: A new hypoxia imaging agent with high membrane permeability and low redox potential. *J Nucl Med* 1997; 38(7): 1155-60.
92. Dearling JL, Lewis JS, Mullen GE et al. Copper bis(thiosemicarbazone) complexes as hypoxia imaging agents: Structure-activity relationships. *J Biol Inorg Chem* 2002; 7(3): 249-59.
93. Dearling JL, Lewis JS, Mullen GE et al. Design of hypoxia-targeting radiopharmaceuticals: Selective uptake of copper-64 complexes in hypoxic cells in vitro. *Eur J Nucl Med* 1998; 25(7): 788-92.
94. Maurer RI, Blower PJ, Dilworth JR et al. Studies on the mechanism of hypoxic selectivity in copper bis(thiosemicarbazone) radiopharmaceuticals. *J Med Chem* 2002; 45(7): 1420-31.
95. Dehdashti F, Mintun MA, Lewis JS et al. In vivo assessment of tumor hypoxia in lung cancer with ^{60}Cu-ATSM. *Eur J Nucl Med Mol Imaging* 2003; 30(6): 844-50.
96. Dehdashti F, Grigsby PW, Mintun MA et al. Assessing tumor hypoxia in cervical cancer by positron emission tomography with ^{60}Cu-ATSM: Relationship to therapeutic response-a preliminary report. *Int J Radiat Oncol Biol Phys* 2003; 55(5): 1233-8.
97. Dehdashti F, Grigsby PW, Lewis JS et al. Assessing tumor hypoxia in cervical cancer by PET with ^{60}Cu-labeled diacetyl-bis(n4-methylthiosemicarbazone). *J Nucl Med* 2008; 49(2): 201-5.
98. Grigsby PW, Malyapa RS, Higashikubo R et al. Comparison of molecular markers of hypoxia and imaging with ^{60}Cu-ATSM in cancer of the uterine cervix. *Mol Imaging Biol* 2007; 9(5): 278-83.
99. Lewis JS, Laforest R, Dehdashti F et al. An imaging comparison of ^{64}Cu-ATSM and ^{60}Cu-ATSM in cancer of the uterine cervix. *J Nucl Med* 2008; 49(7): 1177-82.
100. Ramogida CF, Pan J, Ferreira CL et al. Nitroimidazole-containing H2dedpa and H_2CHXdedpa derivatives as potential PET imaging agents of hypoxia with ^{68}Ga. *Inorg Chem* 2015; 54(10): 4953-65.
101. Hoigebazar L, Jeong JM, Choi SY et al. Synthesis and characterization of nitroimidazole derivatives for ^{68}Ga-labeling and testing in tumor xenografted mice. *J Med Chem* 2010; 53(17): 6378-85.
102. Hoigebazar L, Jeong JM, Hong MK et al. Synthesis of ^{68}Ga-labeled DOTA-nitroimidazole derivatives and their feasibilities as hypoxia imaging pet tracers. *Bioorg Med Chem* 2011; 19(7): 2176-81.
103. Fernandez S, Dematteis S, Giglio J et al. Synthesis, in vitro and in vivo characterization of two novel ^{68}Ga-labelled 5-nitroimidazole derivatives as potential agents for imaging hypoxia. *Nucl Med Biol* 2013; 40(2): 273-9.
104. Wu Y, Hao G, Ramezani S et al. [^{68}Ga]-HP-DO3A-nitroimidazole: A promising agent for pet detection of tumor hypoxia. *Contrast Media Mol Imaging* 2015; 10(6): 465-72.
105. Seelam SR, Lee JY, Lee YS et al. Development of ^{68}Ga-labeled multivalent nitroimidazole derivatives for hypoxia imaging. *Bioorg Med Chem* 2015; 23(24): 7743-50.
106. Mittal S, Sharma R, Mallia MB, Sarma HD. ^{68}Ga-labeled PET tracers for targeting tumor hypoxia: Role of bifunctional chelators on pharmacokinetics. *Nucl Med Biol* 2021; 96-97: 61-7.
107. Bresser PL, Vorster M, Sathekge MM. An overview of the developments and potential applications of ^{68}Ga-labelled PET/CT hypoxia imaging. *Ann Nucl Med* 2021; 35(2): 148-58.
108. Horsman MR, Mortensen LS, Petersen JB et al. Imaging hypoxia to improve radiotherapy outcome. *Nat Rev Clin Oncol* 2012; 9(12): 674-87.
109. Guise CP, Mowday AM, Ashoorzadeh A et al. Bioreductive prodrugs as cancer therapeutics: Targeting tumor hypoxia. *Chin J Cancer* 2014; 33(2): 80-6.
110. McKeage MJ, Jameson MB, Ramanathan RK et al. PR-104 a bioreductive pre-prodrug combined with gemcitabine or docetaxel in a phase ib study of patients with advanced solid tumours. *BMC Cancer* 2012; 12: 496.
111. McKeage MJ, Gu Y, Wilson WR et al. A phase i trial of PR-104, a pre-prodrug of the bioreductive prodrug PR-104a, given weekly to solid tumour patients. *BMC Cancer* 2011; 11: 432.
112. Cardenas-Rodriguez J, Li Y, Galons JP et al. Imaging biomarkers to monitor response to the hypoxia-activated prodrug TH-302 in the MiaPaCa2 flank xenograft model. *Magn Reson Imaging* 2012; 30(7): 1002-9.
113. Liu Q, Sun JD, Wang J et al. Th-302, a hypoxia-activated prodrug with broad in vivo preclinical combination therapy efficacy: Optimization of dosing regimens and schedules. *Cancer Chemother Pharmacol* 2012; 69(6): 1487-98.
114. Lu X, Kang Y. Hypoxia and hypoxia-inducible factors: Master regulators of metastasis. *Clin Cancer Res* 2010; 16(24): 5928-35.
115. Ling CC, Humm J, Larson S et al. Towards multidimensional radiotherapy (MD-CRT): Biological imaging and biological conformality. *Int J Radiat Oncol Biol Phys* 2000; 47(3): 551-60.
116. Supiot S, Lisbona A, Paris F et al. "Dose-painting": Myth or reality? *Cancer Radiother* 2010; 14(6-7): 554-62.
117. Bentzen SM, Gregoire V. Molecular imaging-based dose painting: A novel paradigm for radiation therapy prescription. *Semin Radiat Oncol* 2011; 21(2): 101-10.
118. Busk M, Overgaard J, Horsman MR. Imaging of tumor hypoxia for radiotherapy: Current status and future directions. *Semin Nucl Med* 2020; 50(6): 562-83.
119. Thorwarth D, Monnich D, Zips D. Methodological aspects on hypoxia pet acquisition and image processing. *Q J Nucl Med Mol Imaging* 2013; 57(3): 235-43.
120. Thorwarth D, Eschmann SM, Paulsen F, Alber M. A kinetic model for dynamic [^{18}F]-FMISO pet data to analyse tumour hypoxia. *Phys Med Biol* 2005; 50(10): 2209-24.
121. Souvatzoglou M, Grosu AL, Roper B et al. Tumour hypoxia imaging with [^{18}F]FAZA PET in head and neck cancer patients: A pilot study. *Eur J Nucl Med Mol Imaging* 2007; 34(10): 1566-75.
122. Mortensen LS, Buus S, Nordsmark M et al. Identifying hypoxia in human tumors: A correlation study between ^{18}F-FMISO pet and the eppendorf oxygen-sensitive electrode. Acta Oncol 2010; 49(7): 934-40.

123.Gagel B, Reinartz P, Dimartino E et al. PO_2 polarography versus positron emission tomography ([^{18}F] fluoromisonidazole, [^{18}F]-2-fluoro-2'-deoxyglucose). An appraisal of radiotherapeutically relevant hypoxia. *Strahlenther Onkol* 2004; 180(10): 616-22.
124.Gagel B, Piroth M, Pinkawa M et al. Po polarography, contrast enhanced color duplex sonography (CDS), [^{18}F] fluoromisonidazole and [^{18}F] fluorodeoxyglucose positron emission tomography: Validated methods for the evaluation of therapy-relevant tumor oxygenation or only bricks in the puzzle of tumor hypoxia? *BMC Cancer* 2007; 7: 113.
125.Hoigebazar L, Jeong JM, Lee JY et al. Syntheses of 2-nitroimidazole derivatives conjugated with 1,4,7-triazacyclononane-n,n'-diacetic acid labeled with F-18 using an aluminum complex method for hypoxia imaging. *J Med Chem* 2012; 55(7): 3155-62.
126.Lyng H, Malinen E. Hypoxia in cervical cancer: From biology to imaging. Clinical and Translational Imaging. *Clin Transl Imaging* 2017; 5(4): 373-88.
127.Wykoff CC, Beasley NJ, Watson PH et al. Hypoxia-inducible expression of tumor-associated carbonic anhydrases. *Cancer Res* 2000; 60(24): 7075-83.
128.Wykoff CC, Beasley N, Watson PH et al. Expression of the hypoxia-inducible and tumor-associated carbonic anhydrases in ductal carcinoma in situ of the breast. *Am J Pathol* 2001; 158(3): 1011-9.
129.Pastorekova S, Gillies RJ. The role of carbonic anhydrase ix in cancer development: Links to hypoxia, acidosis, and beyond. *Cancer Metastasis Rev* 2019; 38(1-2): 65-77.
130.Doss M, Zhang JJ, Belanger MJ et al. Biodistribution and radiation dosimetry of the hypoxia marker ^{18}F-HX4 in monkeys and humans determined by using whole-body PET/CT. *Nucl Med Commun* 2010; 31(12): 1016-24.
131.Doss M, Kolb HC, Walsh JC et al. Biodistribution and radiation dosimetry of the carbonic anhydrase ix imaging agent [^{18}F]VM4-037 determined from PET/CT scans in healthy volunteers. *Mol Imaging Biol* 2014; 16(5): 739-46.
132.Dubois L, Douma K, Supuran CT et al. Imaging the hypoxia surrogate marker ca ix requires expression and catalytic activity for binding fluorescent sulfonamide inhibitors. *Radiother Oncol* 2007; 83(3): 367-73.
133.Dubois LJ, Niemans R, van Kuijk SJ et al. New ways to image and target tumour hypoxia and its molecular responses. *Radiother Oncol* 2015; 116(3): 352-7.
134.Wanandi SI, Ningsih SS, Asikin H et al. Metabolic interplay between tumour cells and cancer-associated fibroblasts (CAFS) under hypoxia versus normoxia. *Malays J Med Sci* 2018; 25(3): 7-16.
135.Kugeratski FG, Atkinson SJ, Neilson LJ et al. Hypoxic cancer-associated fibroblasts increase NCBP2-AS2/HIAR to promote endothelial sprouting through enhanced VEGF signaling. *Sci Signal* 2019; 12(567): eaan8247.
136.Simkova A, Busek P, Sedo A, Konvalinka J. Molecular recognition of fibroblast activation protein for diagnostic and therapeutic applications. *Biochim Biophys Acta Proteins Proteom* 2020; 1868(7): 140409.
137.Kratochwil C, Flechsig P, Lindner T et al. ^{68}Ga-FAPI PET/CT: Tracer uptake in 28 different kinds of cancer. *J Nucl Med* 2019; 60(6): 801-5.
138.Giesel FL, Kratochwil C, Lindner T et al. ^{68}Ga-FAPI PET/CT: Biodistribution and preliminary dosimetry estimate of 2 DOTA-containing FAP-targeting agents in patients with various cancers. *J Nucl Med* 2019; 60(3): 386-92.